Magnetospheric Electric Fields Deduced from Drifting Whistler Paths

D. L. CARPENTER, KEPPLER STONE, JAN C. SIREN, AND T. L. CRYSTAL

Radioscience Laboratory, Stanford University
Stanford, California 94305

The amplitude of the E-W component E_w of the convection electric field in the nightside magnetosphere has been inferred from the observed cross-L motions of whistler ducts within the plasmasphere. Several ducts distributed over 1–2 R_E in L space and over ±15° around the longitude of the Eights, Antarctica, whistler station have been tracked simultaneously. The method appears capable of resolving fluctuations in E_w with period $T \sim 15$ min and rms amplitude as low as 0.05 mv/m. For variations with $T > 1$ hour the method has a sensitivity of the order of 0.01 mv/m. Three case studies are presented, two of which illustrate convection activity associated with relatively isolated substorms. In these two cases E_w reversed from westward to eastward for a period following the decay of substorm bay activity. In the third case the substorm bay activity was prolonged, and E_w remained westward and at enhanced levels until local dawn. Evidence was found that, at least in a limited longitudinal sector, perturbing substorm E_w fields can penetrate deep within the plasmasphere. In two of the case studies comparisons of E_w and the interplanetary magnetic-field θ component show evidence of a possible relation based on brief ($\leq$1 hour) southward excursions but not on long preceding southward events. The growth of E_w can take the form of an initial brief (<15 min) positive surge followed by a larger surge that is simultaneous with the most active phase of the substorm. Certain of the pronounced increases in E_w were found to be coincident with activation or spreading of electrojet or auroral activity. In one instance low-amplitude (<0.1 mv/m) presubstorm fluctuations in E_w with periods of the order of 30 min were found to correlate closely with ground-observed midlatitude fluctuations in the magnetic H component. Calculated values of E-field power spectral density from the tracking of two long-lived (~6 hours) whistler paths reveal considerable fine structure. The falloff with frequency roughly as f^{-2} agrees approximately with results from balloons, but the calculated spectral amplitudes appear lower than the balloon results by a factor of ~4. The amplitudes from whistlers appear to be within the range identified by other workers as sufficient to drive radial diffusion in the radiation belts. The present research agrees with balloon measurements on the general presence of a westward field during substorms, but there is apparent disagreement on a number of details, including the post-substorm reversal in E_w.

Substorm-associated convection electric fields in the nightside magnetosphere are sometimes described in terms of a model in which a southward turning of the interplanetary magnetic field is accompanied by an enhanced approximately uniform dawn-dusk electric field. Such a model may be useful in some average sense and may well apply to certain phenomena at relatively high latitudes and in the magnetotail. Near and within synchronous orbit, however, substorm convection reveals complexities whose explanation will require much refinement of existing ideas. For example, enhanced substorm fields appear to be highly localized in longitude [see, for example, *Lezniak and Winkler,* 1970; *McIlwain,* 1971; *Park and Carpenter,* 1970; *Carpenter,* 1970]. Furthermore, as shown in the present research, the relation between southward turning of the interplanetary magnetic field and the E-W component of magnetospheric electric field may not be straightforward, and the electric field may exhibit a post-storm reversal in direction. Much progress has been made in the measurement of magnetospheric electric fields, but a formidable problem in obtaining descriptive information that is suitably detailed both in space and in time remains.

The various experimental techniques for determining E fields currently in use tend to complement one another in regard to the type of information obtained and to the location, duration, and other conditions of the observations

[see recent review by *Maynard,* 1971]. The balloon technique involves observations over extended time periods of the horizontal electric field fringing below the ionosphere. Barium clouds provide a tracer of ion motions for limited periods, usually at ionospheric heights but occasionally at great altitudes. Satellite double-probe experiments in polar orbit provide detailed information on E fields at relatively high latitudes, whereas information derived from low-energy particle surveys at synchronous orbit may be used to infer certain features of substorm electric fields. The whistler method, although it is subject to its own particular limitations, has the advantage of extended time coverage and the remarkable property of being directly involved in the motion of magnetospheric tubes or 'ducts' of ionization. The method has been in use since 1964, although its development and application have been slowed by parallel efforts to investigate the plasmapause. (Such parallel efforts have been beneficial, since the plasmapause appears to serve, although in a complex integral sense, as a means of tracing convection activity in the middle magnetosphere.) Some results from whistlers have been published on the times of occurrence of convection events, on the average sense and velocity of the radial component of flow, and on approximate values of the E-W component of convection electric fields [*Carpenter,* 1966; *Carpenter and Stone,* 1967; *Carpenter et al.,* 1969; *Park and Carpenter,* 1970]. Recently an intensified E-field analysis program has been established to perform case studies and to generally increase the number of reported results. This paper presents some of the first output of that program.

Figure 1 shows a diagram of the whistler method. The dashed curve outlines a region in the magnetic equatorial plane that may be 'observed' from a ground station near $L = 4$ (e.g., Eights or Siple, Antarctica) during periods of favorable multipath whistler activity. The region extends from $L \sim 2.5$ to $L \sim 6$ and to $\pm 15°$ around φ_0, the longitude of the station. The equatorial positions of whistler ducts are labeled A, B, C, and D. (For discussions of whistler propagation in ducts, see *Smith* [1961*a*], *Helliwell* [1965], *Smith et al.* [1960], or *Brice and Smith* [1971].)

The actual distribution of ducts over the viewing area varies in a complicated way with time, magnetic conditions, lightning source activity, etc. On a typical austral-winter day five to ten ducts with equatorial radii distributed over 0.5–2 R_E in L space may be tracked simultaneously from an antarctic station near the 0° geomagnetic meridian. (Activity at other longitudes is being investigated on a cooperative international basis.) Individual ducts can be observed for periods ranging from minutes to hours. The broad-band nature of the records and the high occurrence rate of whistlers (~1–20 per min) facilitates identification of the individual field-aligned paths.

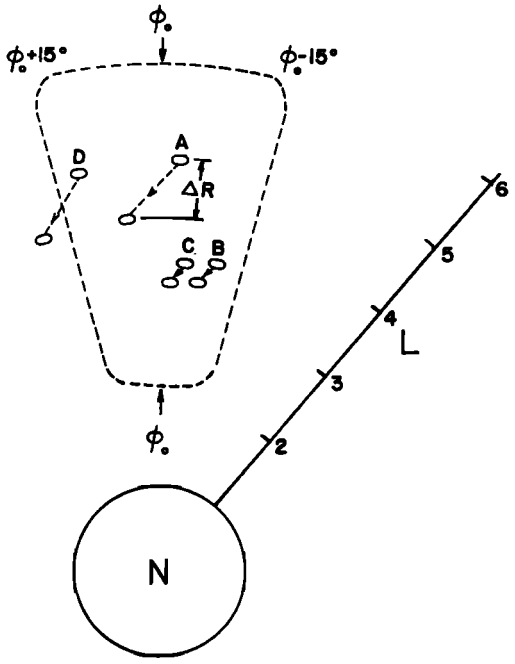

Fig. 1. Diagram of the whistler method of tracking the cross-L motions of whistler ducts. The dashed line outlines the region that a ground station near $L = 4$ is capable of observing. Four representative ducts are labeled A, B, C, and D. The number of whistler ducts actually 'observed' per unit L or φ may vary in a complicated way with both L and φ and with time.

The whistler 'nose' frequency f_n, the frequency of minimum travel time, is approximately proportional to the equatorial magnetic-field strength along the field-aligned whistler duct [see *Smith,* 1961*b*, or *Carpenter and Smith,* 1964]. The whistler travel time at the nose frequency, τ_n, is related to f_n in a manner that

permits either f_n or τ_n to be scaled for information on path position (see the appendix). (τ_n can be visualized as a measure of the length of the field-aligned whistler duct.) If the time of each whistler's causative atmospheric is known, τ_n is usually the easier quantity to scale on frequency-time records. In the present study the causative atmospherics were clearly identifiable on the records. τ_n or an equivalent travel time was scaled, and values of f_n were used to check on the results.

During a convection event ducts undergo apparent displacements with respect to the observing frame of the corotating ground station [see *Carpenter,* 1966, 1970; *Park and Carpenter,* 1970]. These displacements, illustrated in Figure 1, are interpreted as bulk motions of the magnetospheric plasma. For each duct the whistler method identifies ΔR, the radial component of the displacement. Comparison of ΔR values from ducts spaced in L and in φ permits one to make certain inferences about the spatial extent of convection activity.

The present whistler method does not explicitly identify the longitudinal coordinate of a whistler duct. Coarse information on longitude and on longitudinal drift can be obtained from the 'disappearance' of a duct from the view of a station, as for duct D in Figure 1, or from comparison of data recorded at stations separated in longitude by 15°–40°. In future experiments it is hoped that two vector components of duct motion will be determined by radio direction finding of duct endpoints in the ionosphere.

Figure 2 illustrates whistler data from a case study described previously (but in less detail) by *Carpenter and Stone* [1967]. Local midnight at the observing whistler station, Eights, Antarctica, is marked M. The quantity plotted versus time is τ_n^{-1}, which can be visualized as a measure of the inverse length of the whistler's field-aligned path. Successions of points varying in length from tens of minutes to 6 hours represent tracking of individual ducts, typically five or six at a given time. At ~0240 UT the ob-

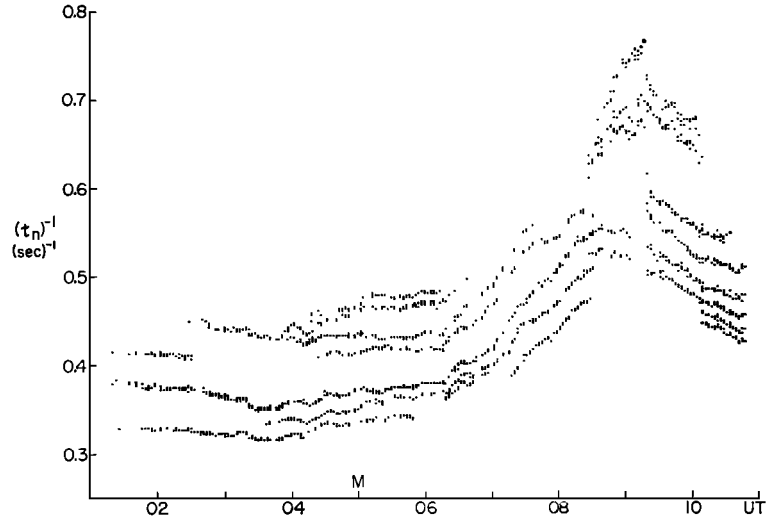

Fig. 2. Graph of the reciprocal of whistler travel time at the nose (τ_n^{-1}) versus time, illustrating convection activity on several whistler paths over a 10-hour period on July 15, 1965, that included an isolated substorm. The sequences of data points represent various ducts tracked for periods ranging from tens of minutes to over 5 hours. The path L values ranged from $L = 3.7$ to 4.5. Negative slope indicates an eastward electric field; positive slope indicates a westward electric field. A substorm began between 0600 and 0700 UT. Local midnight at the observing whistler station (Eights, Antarctica) is indicated by M. The data gap near 0910 UT is due to a magnetic recording-tape change during a period of increased difficulty in determining continuity of whistler paths. Paths tracked after 0910 were not assumed continuous with those tracked before the tape change. Termination of the data near 0200 and 1100 UT reflects corresponding changes in the quality of whistler activity, and it does not reflect gaps in recording.

served ducts were distributed over the range $4.2 < L < 4.8$. Near ~0750 UT the range was $\sim 3.8 < L < 4.2$, and at ~1010 UT it was $4.0 < L < 4.3$.

From the hydromagnetic relation $\mathbf{E} = -\mathbf{v} \times \mathbf{B}$ the westward component of magnetospheric equatorial electric field E_w may be shown to be proportional to the time derivative of τ_n^{-1} through a factor that varies only slightly with L (see the appendix). Hence Figure 2 provides a general indication not only of the variations in E_w with time but also of the extent to which the variations are homogeneous over the $\sim \Delta L = 0.5$ range represented. The values of τ_n^{-1} first show a generally decreasing trend (negative E_w) until about 0330 UT and then a gradually increasing trend (positive E_w) until about 0615 UT. After 0615 larger positive slopes are evident on all paths until about 0900 UT, when the slopes become relatively large and negative. The decreasing trend in τ_n^{-1} continues until the end of the data coverage.

To obtain detailed estimates of E_w, whistler data of the kind illustrated in Figure 2 were differentiated numerically by a method that filters out fluctuations with periods shorter than 10–15 min (see the appendix). Results for several case studies are summarized below. Except as noted, the whistler paths described are within the plasmasphere.

Experimental Results

Event of July 15, 1965

The values of the westward component of magnetospheric electric field deduced from each of the sequences of data points in Figure 2 are presented in superposed fashion in Figure 3. At the top is a transcription of the geomagnetic H component recorded at Byrd, Antarctica ($L \sim 7$). Byrd lags the Eights whistler station by about 1 hour in magnetic local time; hence Byrd H provides a crude indication of magnetic substorm activity near the longitude of Eights. Local midnight at Eights is indicated by an M on the time scale. Hourly AE values for the period July 12–15, 1965, are shown in Figure 4*a*. The period preceding the July 15 interval of interest (horizontal flag) was generally quiet. The last previous substorm activity was relatively weak and occurred roughly 8 hours before the substorm of ~0700 UT on July 15. Sums of Kp on July 12, 13, 14 and 15, were 9, 11, 8 and 17, respectively. Hourly Dst for 0800–0900 UT on July 15 was −3 γ. With reference first to Figure 3 the main features of the E_w activity were as follows:

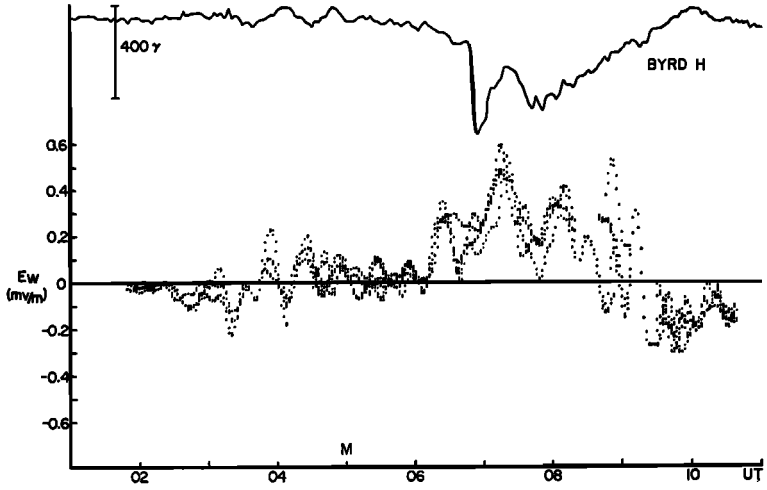

Fig. 3. Values of westward electric field E_w in the magnetosphere near $L = 4$ on July 15, 1965, determined from the data of Figure 2 through smoothing and differentiation. Data from all whistler paths are superposed. The Byrd, Antarctica, H component is shown as a crude indication of magnetic substorm activity near the meridian of the whistler E_w observations. Local midnight at the Eights, Antarctica, whistler station is indicated by M. (Byrd is about 1 hour behind Eights in magnetic local time.)

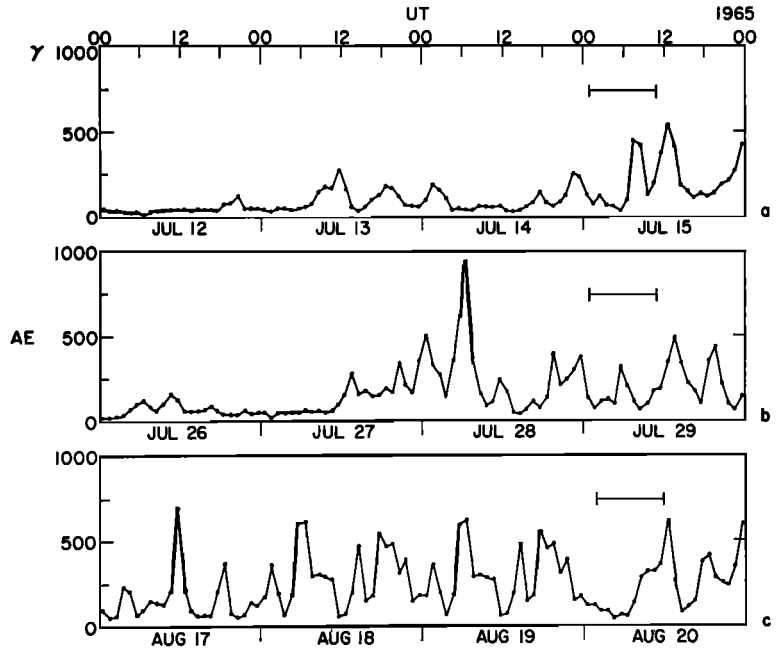

Fig. 4. Hourly *AE* index for several days preceding the three 1965 intervals discussed in the text (horizontal flags). (*a*) and (*b*), Relatively isolated substorm behavior. (*c*) Prolonged substorm activity.

Presubstorm activity. Between 0200 and 0600 UT fluctuations in E_w with rms amplitude ~0.07 mv/m appear to include a strong spectral component with $T \sim 30$ min. During some intervals, e.g., 0400–0430 UT, the fluctuations have similar amplitudes and phases for all the observed whistler paths. At other times, e.g., near 0530 UT, two or more distinctly different curves may appear. Some of the differences in the curves may be due to temporal and spatial structure in E_w and to details of the distribution of whistler ducts (see Figure 1); an additional example of such effects is described below.

Evidence that the presubstorm oscillations are real is provided by Figure 5, which shows detailed similarity between an individual E_w curve from Figure 3 (below) and the H component of the Fredericksburg, West Virginia, magnetometer. Fredericksburg is located within the expected longitudinal viewing range of the Eights whistler station and at $L \sim 3$; the E_w curve represents activity at $L \sim 4.2$. Evidence that the E_w fluctuations penetrated to $L \sim 3$ is presented in Figure 6, which shows a rough similarity between the E_w curve from Figure 5 (solid curve at top of figure) and E_w values obtained near $L = 3.3$ (dotted and dashed curve). (The results for $L \sim 3.3$ and for $L \sim 2.7$ at lower right are more sensitive to measurement errors, and they required more smoothing than the results for $L \sim 4$. This problem is discussed in the appendix.) If it is assumed that there is some form of coupling between the geomagnetic and E_w fluctuations, it is concluded that, within some longitude range near Fredericksburg and Eights, there were coherent presubstorm oscillations in E_w over a range $\Delta L \sim 2$ inward from the plasmapause. (The plasmapause is locally estimated to have been near $L = 5$ in the presubstorm period.)

Figure 3 shows that in the period ~0200–0340 UT the ~1-hour running average E_w was slightly negative (hence eastward) on the various paths, with amplitude <0.1 mv/m. At ~0340 UT, roughly an hour before local midnight, the average field became slightly westward, remaining in this direction on most of the paths through 0600 UT. The illustrative E_w curve in Figure 5 (the lower curve) shows

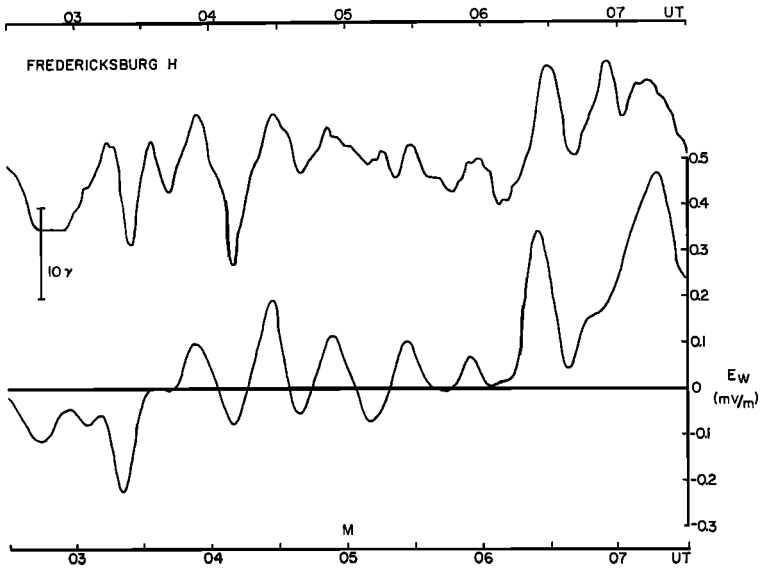

Fig. 5. Comparison of the magnetic H component on July 15, 1965, at Fredericksburg, West Virginia ($L \sim 3$), and the electric field at $L \sim 4.2$ in the magnetosphere determined near the longitude of Fredericksburg. Approximate local midnight at both observing stations is indicated by an M on the lower scale. Most of the period indicated precedes substorm activity that developed between 0600 and 0700 UT. See Figures 3 and 6 for additional information on the E-field envelope.

an average value of ~0.03 mv/m westward from 0400 to 0600 UT. Relatively large-scale coherence of the running average field is suggested by the comparison of measurements at $L \sim 3.3$ and $L \sim 4.2$ in Figure 6. The shift from negative to positive E_w near ~0340 UT is particularly clear.

Development of the substorm. Recently S. Akasofu (private communication, 1971) has compared results from this research with all-sky-camera data and magnetometer records. In general, the results are complex and appear to warrant separate treatment; some of the results are mentioned briefly in the following paragraphs.

At about 0615 UT on July 15 (Figures 2 and 3) there was a sharp increase in E_w on all paths near $L = 4$. A less-well-defined increase appears in the data from $L \sim 3$ (Figure 6). Near $L = 4$ (Figures 3 and 5) the field reached half its initial peak of about 0.3 mv/m within less than 7 min. This peak was then followed on all but one of the observed paths by a deep minimum lasting about 10 min.

The surge of E_w at ~0615 UT was coincident with an initial activation of electrojet currents as observed from Churchill, Byrd, College, and Barrow (S. Akasofu, private communication, 1971).

Active phase of the substorm. After 0640 UT there was a generally increasing trend in E_w on all paths, a relatively well-defined maximum of ~0.5 mv/m occurring at ~0715 UT. Sharp negative bays began at Churchill and Byrd at 0627 and 0645 UT, respectively. The differences in detail at these two stations (in conjugate hemispheres but less than 1 hour apart in magnetic local time) suggest localization of the electrojet during an early stage of the substorm (S. Akasofu, private communication, 1971). The differences may have their counterpart in some of the differences in the E_w envelopes in the period 0630–0700 UT (Figure 3).

After 0640 UT the E_w envelopes continued to exhibit pronounced fluctuations. Between about 0640 and 0830 UT the 1-hour running average of the E_w field was about 0.25 mv/m near $L = 4$. Near $L = 3$ (Figure 6) there is also indication of enhanced average fields at this time.

Recovery phase of the substorm. At 0830–0900 UT, as the bay activity at Byrd dimin-

ished (Figure 3), the E-W field reversed and became relatively large and eastward. One-hour running average values reached ~0.2–0.3 mv/m eastward and then decreased. Figure 6 provides evidence of coherence of the average field over a wide L range during the period 0900–1030 UT.

The complexity of Figure 3 between ~0840 and 0920 UT is partly due to the simultaneous detection of both inward and outward motions near $L = 4$. Beginning at about 0830 UT several paths were detected near but apparently outside the plasmapause (Figure 2, upper group of data points). These paths showed evidence of inward motion (increasing τ_n^{-1}) until 0900–0910 UT, whereas two of the paths in the lower group exhibit clear evidence of a reversal in flow direction at ~0840 UT. Thus Figure 3 shows eastward fields of ~0.1 mv/m near 0900 UT and also westward fields in the range 0.3–0.5 mv/m. After 0920 UT the observable motion of both groups of traces in Figure 2 is outward, corresponding to the eastward fields indicated in Figure 3.

By 0830 UT the plasmasphere traces (main group in Figure 2) had been under observation for some time. It is possible that they had already drifted eastward within the viewing sector, in the manner indicated schematically in Figure 1. Such a drift would be consistent with the cross-L inward electric fields that are observed to accompany westward substorm fields [*Mozer and Serlin*, 1969; *Mozer and Manka*, 1971]. The paths first detected just beyond the plasmapause at ~0830 UT (~0330 MLT) may then have been located on the westward or midnight side of the viewing sector, well separated from the other traces, although at a similar L position. The delayed reversal in flow direction of the group appearing at ~0830 UT may be evidence that the decaying westward field persisted longest near midnight.

Additional notes on the plasmapause. The plasmapause position appears to provide a complicated integral measure of convection activity. From indirect evidence at ~0600 UT, based on propagation within the plasmasphere [see *Carpenter*, 1966], and from direct evidence at ~0830 UT, based on propagation through both low- and high-density regions, the plasmapause is inferred to have been displaced inward through $\Delta L \cong 0.6$ during the early and active phases of the substorm. After 0830 UT electron-density structure appeared in the form of multiple density levels outside the plasmasphere. For example, the upper group of data points in Figure 2 represents a region of electron density reduced from typical plasmasphere levels by a factor of about 2. Other data from slightly larger L values indicated 'plasma-trough-like' concentrations a factor of ~10 below the plasmasphere level. These traces were not sufficiently well defined or persistent for detailed analysis of convection effects.

Event of July 29, 1965. Figure 7 shows another relatively isolated substorm event from 1965. The format is similar to that of Figure 3, except that individual E_w curves from repre-

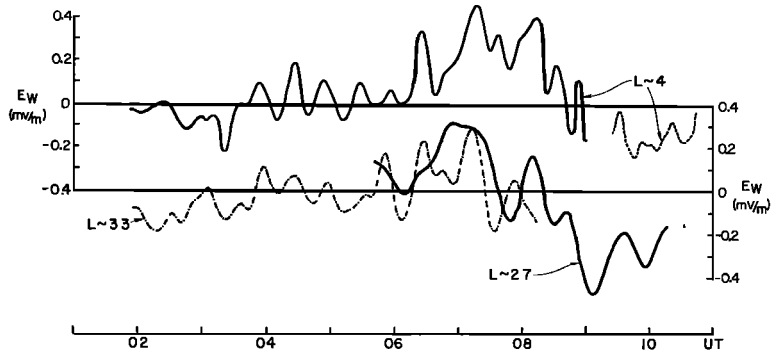

Fig. 6. Comparison of E_w observed in different L ranges during the convection event of July 15, 1965. The curves for $L \sim 3.3$ and $L \sim 2.7$ involve smoothing that is in addition to the smoothing required at $L = 4$, owing to an increase as L decreases in the effects of experimental error (see the appendix). The particular whistler paths illustrated were chosen for their relatively long duration and for quality of definition on the spectrographic records.

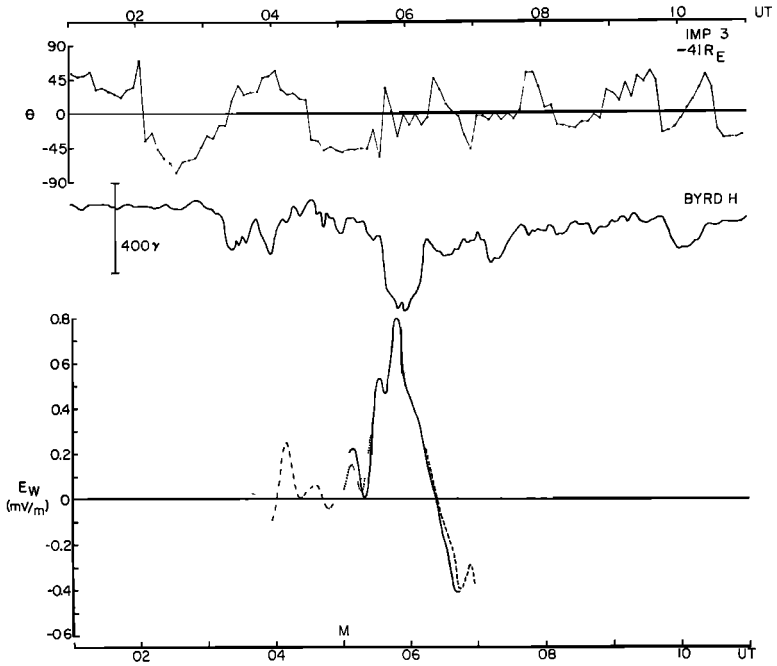

Fig. 7. Temporal variations of the westward component of magnetospheric equatorial electric field near $L = 4$ during an isolated substorm on July 29, 1965. Local midnight at the observing whistler station (Eights, Antarctica) is marked M. Results from several whistler paths are compared to the Byrd, Antarctica, geomagnetic H component and to Imp 3 data on θ, the interplanetary magnetic-field direction with respect to the ecliptic plane (see the top panel). Presentation of θ in coordinates reflecting the tilt of the earth's dipole axis would result in small negative increases up to a maximum of about 10° in the plotted values. These corrections were not believed to be necessary in the context of the present paper.

sentative whistler ducts are shown and Imp 3 5.46-min average values of θ, the angle of the interplanetary magnetic field vector with respect to the solar ecliptic plane, are added at the top. (Imp 3 was inside the magnetosphere during the July 15 study.) Hourly AE values for 3 days preceding the period of Figure 7 are plotted in Figure 4*b*. The period of interest (horizontal flag) occurs 36 hours following the beginning of a weak magnetic storm and during a period of regular but relatively well-separated surges of activity. Sums of Kp on July 26, 27, 28, and 29 were 7, 16, 23 and 20, respectively. Hourly Dst for 0500–0600 UT on July 29 was -6 γ.

The E_w curves in Figure 7 represent the outer plasmasphere. At ~0400 UT the L value represented is ~4.6. Between 0600 and ~0700 UT the path movements were near $L = 3.7$. In this case study and in the following one the number of well-defined components in a typical whistler was less than in the July 15 case, hence the smaller number of E_w curves in Figures 7 and 8. In all the case studies, except at ~0910 UT on July 15, interruptions and terminations of E_w curves identify corresponding interruptions or changes in whistler activity suitable for scaling, and they do not indicate gaps in recording.

Some features of the July 29 case are as follows:

Near 0400 UT there was a brief westward increase that may have been associated with the substorm indicated by the Byrd magnetometer. The field then fluctuated around a small average level until ~0500 UT, when another brief westward event occurred. The field then dropped to near zero, and at 0520 UT a pronounced westward increase began.

As in the July 15 event, there was evidence of electrojet activations closely correlated in time with the E_w increases but exhibiting complex

evidence of localization and spreading (S. Akasofu, private communication, 1971). At Byrd, for example, there was a small (<100 γ) bay near 0500 UT (Figure 7). Another bay began at ~0525 UT, as the pronounced E_w increase developed. (Near 0525 UT there was also a sudden activation of auroras observed from Byrd.) Near 0540 UT there was a further steep decrease in Byrd H as the E_w curve surged to its highest level.

E_w reached a maximum of ~0.8 mv/m near the bay minimum and decayed rapidly as the Byrd H component recovered. As in the July 15 event, the increases in E_w to substorm levels reached half maximums within about 7 min (with further analysis more precise estimates of rise time should be possible). The corresponding rates of later decay and reversal are difficult to summarize, but in the present situation (Figure 7) they appear to involve times of the order of 10 min.

A reversal of the field immediately followed the large westward event. The initial peak of the eastward field is ~0.4 mv/m, less than the substorm westward maximum but larger than typical prestorm magnitudes.

The Imp 3 results on θ in Figure 7 represent a SEP angle of 296°, corresponding to the ~1600 LT meridian. Relatively brief southward turnings of θ at ~0205, 0435, 0650, and 0945 UT appear to be correlated with a series of electrojet activations at Byrd. The large E_w increase appears to be related to the interplanetary event beginning at ~0435 UT. There is an apparent delay of 15–20 min between the southward turning of θ and the initial E_w increase near 0500 UT and a delay of 40–50 min until the main E_w increase. The latter delay occurs during a period of irregular recovery of θ from a relatively steady southward orientation.

Synoptic and continuous whistler data indicate that the plasmasphere remained relatively large on July 28 and 29, the average equatorial radius being ~5 R_E. As in the July 15 event, there was evidence of inward plasmapause displacement to $L \sim 4$ during the substorm and also some evidence that this effect was limited in time and space in a manner consistent with the limited duration and reversal of the electric field.

Event of August 20, 1965. The two events described above are representative of a large class of substorm-associated events in which the cross-L inward convection is followed by an outward drift. There is also another large class of events, smaller than the first, characterized by cross-L inward drifts that persist until near dawn. Figure 8 shows an example of this behavior from August 20, 1965. The format is similar to that of Figure 7. Two of the best-defined whistler traces are represented by the solid and the dashed curves. The curves represent duct displacements from $L \sim 3.7$ at 0330 UT to $L \sim 2.7$ at 1100 UT. The dashed curve, representing activity near $L = 3$, involves a larger amount of smoothing than the full curve (see explanation in the appendix).

Hourly values of the AE index for several days preceding the interval of interest (horizontal flag) are shown in Figure 4c. As for the event of July 29 (Figure 4b), a weak magnetic storm was underway, but in the August event the preceding activity was somewhat more intense and of longer duration. Sums of Kp on August 17, 18, 19, and 20, were 19, 19, 30, and 24, respectively. The minimum hourly Dst during the interval of Figure 8 was −10 γ at 1000–1100 UT. Some of the main features of the event follow.

Prior to 0500 UT (or ~0000 LT) the ~1-hour running average of the field was less than 0.1 mv/m westward. From ~0500 to ~0620 UT the average field was less than 0.1 mv/m eastward. From 0620 until about 0730 UT the average was again westward but at a level somewhat above 0.1 mv/m.

At ~0730 UT (~0230 MLT) the Byrd H component began to decrease gradually but steadily. At this time the E field began a surge to higher westward levels near 0.5 mv/m. The field remained high until about 0920 UT (~0420 MLT) and then continued to be westward with average levels between ~0.1 and 0.2 mv/m until the end of data coverage at 1120 UT (~0620 MLT).

Throughout the period of observation the field exhibited relatively large fluctuations with rms amplitude of the order of 0.07 mv/m and periods in the range 20–60 min, a behavior similar to that of the July 15 event.

The interplanetary magnetic-field angle θ, observed near the ~1400 LT meridian at an SEP angle of 324°, remained northward during

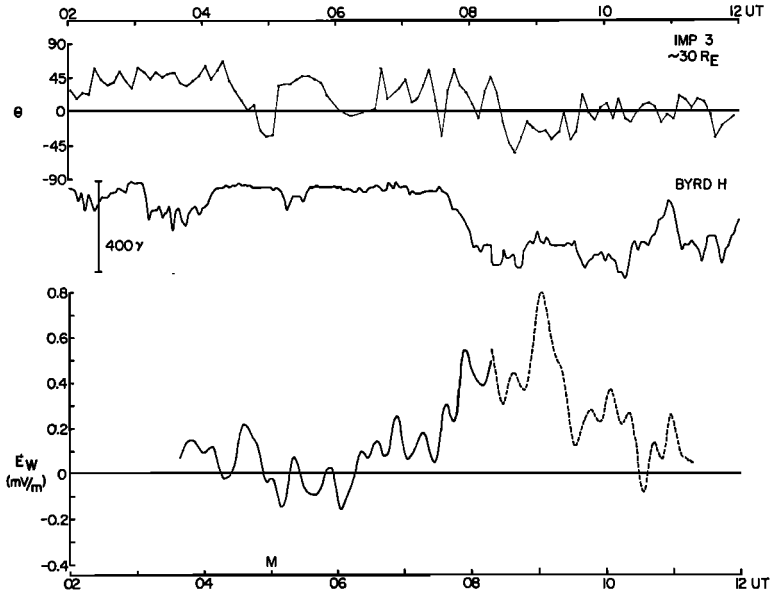

Fig. 8. Temporal variations of the westward component of magnetospheric electric field during a prolonged period of substorm activity that began after local midnight at the whistler station (marked M on the lower scale). The date is August 20, 1965, and the format is the same as in Figure 7, involving the Byrd H component and the Imp 3 interplanetary magnetic-field angle θ. The whistler paths represented were tracked from $L \sim 3.7$ at 0330 UT to $L \sim 2.7$ at 1100 UT.

a bay event at Byrd near 0300 UT. A brief southward excursion near 0500 UT was followed by a small bay event at Byrd, but there was no evident change in E_w. The decrease in θ near 0600 was followed by the period of somewhat enhanced E_w from 0620 to 0730 UT. The sharp brief southward turning in θ at ~0730 UT was followed by the steep rise in E_w to the ~0.5-mv/m level. Whatever the real $E_w - \theta$ relation was, it appears to have partly been based on short 'triggering' effects.

E-field and Byrd H signatures of the general type shown in Figure 8 usually occur in the early part of moderate to weak magnetic storms. Magnetic bay activity at $L \sim 7$ is prolonged (compare Byrd H in Figures 3 and 7 with Byrd H in Figure 8), and inward drifts occur throughout much of the local-time sector from midnight to dawn. Such periods are usually characterized by pronounced reductions in average plasmapause radius. In the August 20 event the plasmapause as observed from Eights was reduced from $L > 4.4$ at 2230 MLT to $L \sim 3$ near local dawn.

Some details of the power spectrum of the westward electric field. To provide a preliminary view of the power spectrum of the measured electric fields, a Fourier analysis was made of E_w envelopes from two whistler paths, both of which were tracked continuously over roughly 6-hour periods. The two E_w envelopes, one from July 15, 1965, and the other from August 20, 1965, are shown by the solid curves in the top panel of Figure 6 and in Figure 8, respectively. Figures 9 and 10 show the calculated power spectra plotted in units of $(\text{mv/m})^2$ Hz^{-1} versus frequency in cycles per hour. Also plotted for comparison is the curve obtained from balloon E-field measurements by *Mozer* [1971*a*] and mapped to the equatorial plane. In both instances Mozer's curve is shown for the appropriate level of magnetic activity. The spectral amplitudes from whistlers fall off roughly as f^{-3} up to a frequency of about 4 cycles per hour, above which the effect of the filtering applied to the data causes a steep dropoff. The vertical flag on Mozer's curve indicates the standard deviation of curves fitted to the data from various spaced stations and from various days. For a single several-hour observa-

tion from a given location, the variability is substantially less.

Either in a least-squares sense or on the basis of a fit weighted to the peak amplitudes, the whistler results fall below the balloon-data curve by a factor of roughly 4. In spite of this result the fluctuations determined from whistlers appear to be within the range identified by *Cornwall* [1972] as sufficient to drive radial diffusion in the radiation belts.

The variations in spectral amplitude are relatively large in comparison with those found from the balloon experiments. The pronounced peaks at 28 and 56 min in Figure 9 correspond to the relatively pure presubstorm oscillations discussed earlier.

CONCLUDING REMARKS

The whistler method of measuring the E-W component of magnetospheric electric field (E_w) is under continuing development. For the present the method appears capable of resolving fluctuations in E_w with a period of 15 min and an rms amplitude as low as 0.05 mv/m at the magnetic equator and near $L = 4$. For longer-period variations in E_w, e.g., with $T > 1$ hour, the method has a sensitivity of about 0.01 mv/m and an accuracy limited by protonosphere-ionosphere coupling effects and ionospheric density changes that introduce dc offsets of the order of 0.01 mv/m (see the appendix).

The E_w fields; penetration to low L. In the July 15, 1965, event described above, similar E-W E-fields were observed at $L \sim 2.7$ and at $L \sim 4$ when the plasmapause was near $L = 4.5$. This observation confirms previous reports that perturbing substorm convection fields can penetrate the plasmasphere [*Carpenter and Stone*, 1967, 1968; *Mozer*, 1971*a*], and it is consistent with the observation of *Park and Meng* [1971] that changes occur in the midlatitude nightside F region during substorms, apparently in conjunction with convection events in the magnetosphere. Further whistler studies at $L \leq 3$,

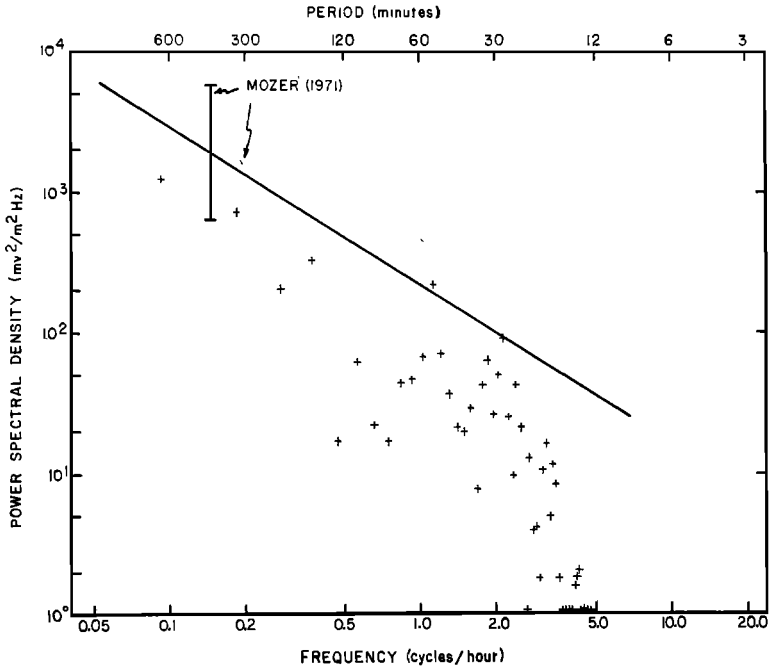

Fig. 9. Calculated power spectral density of the westward component of magnetospheric equatorial electric field, plotted versus frequency in cycles per hour and period in minutes. The calculations represent the E-field envelope of 0250–0820 UT and 2150–0320 LT on July 15, 1965, shown in the top panel of Figure 6 (solid curve). $L \sim 4.5$–3.8. For comparison, *Mozer's* [1971*a*] results from balloon E-field measurements for a corresponding level of magnetic activity are given (solid line).

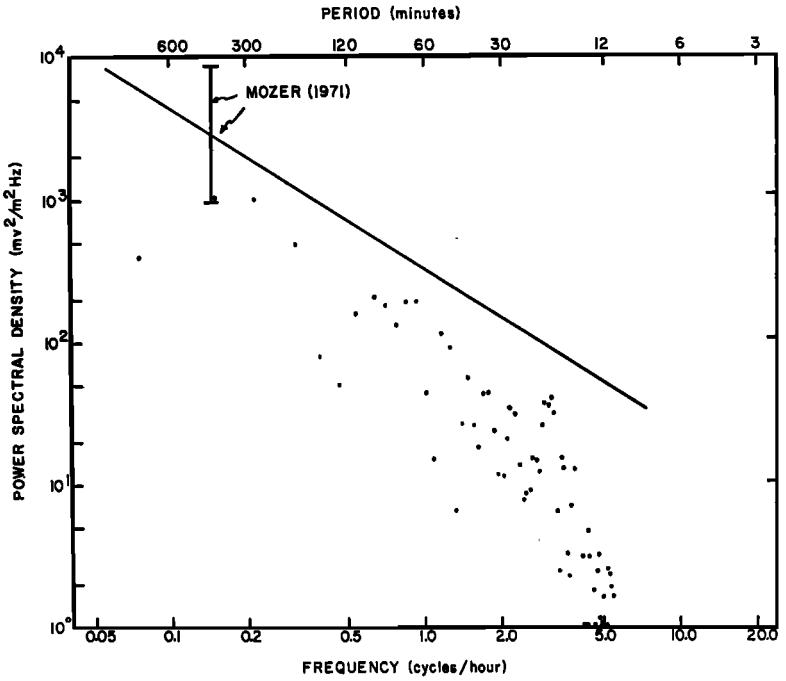

Fig. 10. Calculated power spectral density of the westward component of magnetospheric equatorial electric field, plotted versus frequency in cycles per hour and period in minutes. The calculations represent the E-field envelope of ~0330–0830 UT and ~2230–0330 LT on August 20, 1965, shown by the solid curve in Figure 8. $L \sim 3.6$–3.1. For comparison the solid line represents *Mozer's* [1971*a*] results from balloon E-field measurements for a corresponding level of magnetic activity (see the text for details).

augmented by phase-path measurements on fixed-frequency signals, should provide additional information on the penetration of E fields to low latitudes.

West to east reversal of the field. During the two 'isolated' substorms illustrated in this paper, the azimuthal E field turned from westward to eastward in a later stage of the event. Since the typical 'quiet time' (between substorm) direction of observed cross-L drift is inward in the 2300–0300 LT sector and outward after ~0300 LT [*Carpenter and Stone,* 1968], the in-out sequence of isolated substorm flow appears to be a kind of temporal enhancement of the normal flow pattern.

Longitudinal structure in E_w. Earlier whistler reports have noted the tendency of enhanced substorm-associatd cross-L inward drifts to be confined to the post-2300 LT sector [*Park and Carpenter,* 1969; *Carpenter,* 1970]. The simultaneous detection of inward and outward drifts late in the relatively isolated event of July 15 may be additional evidence of a confinement of certain enhanced substorm fields to a limited longitudinal range near midnight. Evidence of such a confinement has been discussed by, among others, *Lezniak and Winkler* [1970]. Thus it appears that substorm E fields near $L = 4$ can not be described in terms of a more or less uniformly enhanced cross-tail field. Instead, the effect becomes more like that of a localized 'injection,' as discussed (for synchronous orbit) by *DeForest and McIlwain* [1971] and *McIlwain* [1971].

Fluctuations in E_w with an rms amplitude of ~0.1 mv/m and a period of <1 hour were observed throughout two 10-hour periods. In the July 15 event a detailed similarity was found between $T \sim$ 30-min presubstorm oscillations in E_w at $L = 3$–4 and oscillations in the magnetic H component at a midlatitude observatory. The nature of the coupling between the H and E_w variations is not yet known. Further study may reveal a relation between these effects and nat-

ural resonances of the geomagnetic tail (see, for example, *Patel* [1968] and *Ershkovich and Nusinov* [1971]).

Comparison of prolonged and isolated convection events. In contrast with the isolated events, the prolonged substorm event of August 20, 1965, involved the following factors: (1) a relatively long period of positive E_w (in such instances the region of enhanced inward convection appears to spread toward the dawn sector), (2) no predawn reversal of E_w, and (3) small plasmasphere size. The time integral of E_w between ~2300 and 0600 MLT appears to provide a measure of the reduction in plasmasphere size. The plasmapause was observed at $L \sim 3$ in the forenoon sector following the August 20 nightside event; in the other two instances it was in the range $L = 4$–5.

The difference between isolated and prolonged convection events may not involve a pronounced difference in the rms value of E_w. Of greater importance may be the mentioned difference in $\int E_w dt$ and the difference in spatial extent of the convection activity.

Relations between E_w and the interplanetary-field angle θ from Imp 3 are complex. In the July 29 isolated event the main E_w event appears identified with an hour-long southward turning of θ, although the main part of the E_w event develops as θ becomes more positive. In the event of August 20, the interplanetary field shows a generally southward trend at the time of the prolonged bay and E_w event. A possible E_w-θ relation involves a series of relatively brief southward excursions, which may individually have triggered processes in the magnetosphere.

Because of the evident variety and complexity of substorms and the associated E fields, it is difficult to compare whistler results based on magnetospheric convection with balloon-borne E-field measurements below the ionosphere. Some simultaneous data exist and are being processed, but good overlap in both L and longitude has not yet been achieved. Both experiments appear to detect rises in E_w at times of activation of substorm-associated ionospheric currents or auroral activity [e.g., *Mozer and Manka*, 1971]. Both experiments also observe a westward field during the most active phase of the substorm [*Mozer*, 1971*b*]. The balloon results suggest that E_w is relatively steady after it is activated [*Mozer*, 1971*b*], whereas the whistler results indicate progressive increases that appear to reflect changes and possibly spreading in areas of activation in the ionosphere. The whistler and balloon measurements appear to disagree on the reversal of the field from westward to eastward following isolated substorms. This effect has not appeared as a regular feature in the balloon results but has been inferred from the low-energy particle survey at synchronous orbit by *McIlwain* [1971]. (What may be a related field reversal has been reported from rocket measurements near an auroral arc by *Choy and Arnoldy* [1971].) The whistler and balloon experiments agree on the general shape of the E-field fluctuation spectrum [see *Mozer*, 1971*a*] but appear to disagree by a factor of ~4 on power spectral amplitudes and also on the presence of detailed structure in the fluctuation spectra.

If there is a growth phase in the two isolated E-field events reported above, it has a duration of ~15–25 min and involves an enhancement of E_w to a level less than that reached in the active phase. E_w may then decay to near zero before the following larger increase. A possible growth phase in the prolonged August 20 event occurred from 0620 to 0730 UT (Figure 8), when a moderately enhanced fluctuating E_w envelope was observed for over an hour before a large further increase. In all three case studies certain clear increases in E_w were coincident with activations or significant changes in auroral and/or electrojet activity as observed on the ground. More quantitive and detailed analyses of these relations are planned.

A new program of intensive whistler measurements that will last several years will begin in early 1972 at Siple, Antarctica (76°S, 84°W, $L \sim 4$), near Eights, Antarctica, where the data discussed in this paper were recorded. On the basis of these new measurements and associated measurements at other longitudes, much detail on magnetospheric convection under both quiet and disturbed conditions should become available.

APPENDIX

Relation of $d(\tau_n^{-1})/dt$ and E_w. A centered dipole is used to represent the geomagnetic field. It is assumed that the electron content of a tube of ionization remains constant during a convection event. (Experimental evidence in

support of this assumption is given by *Park and Carpenter* [1970] and by K. Stone (unpublished research, 1967). It is then possible to show empirically that for a convecting whistler path

$$\tau_n f_n^{2/3} \simeq \text{const} = C_0 \qquad (1)$$

during a convection event, where τ_n is travel time at the whistler nose frequency f_n. This 'constant-content' relation has been verified experimentally in unpublished work at Stanford by C. Park and by K. Stone. The relation is implicit in the work of *Angerami* [1966, p. 11] and has been derived by C. G. Park (unpublished manuscript, 1971).

Another relation assumes proportionality between the nose frequency and equatorial gyrofrequency [*Smith*, 1960, 1961*b*; *Angerami*, 1966], as follows:

$$f_n = k f_{H_{eq}} = k f_{H_0}(R_0/R)^3 \qquad (2)$$

where $k \sim 0.38$ for a diffusive equilibrium model of the field-line distribution of ionization, and $f_{H_{eq}}$ and f_{H_0} are the equatorial electron gyrofrequencies at geocentric distances R and R_0 (earth's surface), respectively.

Specializing the hydromagnetic drift relation $\mathbf{v} = \mathbf{E}\times\mathbf{B}/B^2$ to the magnetic equator, we obtain (in mks units)

$$dR/dt = -(E_w/B_0)(R_0/R)^{-3} \qquad (3)$$

where B_0 represents the geomagnetic-field strength at the earth's surface and E_w is the westward component of the magnetospheric electric field.

The constant C_0 in (1) is evaluated from measurements of τ_n (in sec) and f_n (in kHz) at some time during the convection event: from (1), (2), and (3) we obtain

$$E_w = 2.07 C_0\, d(\tau_n^{-1})/dt \quad v/m \qquad (4)$$

Within the plasmasphere and beyond $L = 3$, the variations in C_0 from one whistler path to another are usually of the order of 10%, although variations up to a factor of 2 can occur when large-scale density structures are observed within the plasmasphere [e.g., *Park and Carpenter*, 1970].

E_w measurements near $L = 3$. For paths near $L = 3$ the whistler nose frequency may not be detectable, owing to source or propagation effects or to the limited bandwidth (~0–10 kHz) of certain presently available continuous records. In such instances measurements are made at a fixed frequency below the whistler nose, and E_w becomes proportional to the product of $d(\tau^{-1})/dt$ and a function of τ, where τ is travel time at the fixed measurement frequency. Because of the shape of the whistler dispersion curve and the manner in which the curve is transformed in frequency-time space during a convection event, travel time becomes progressively less sensitive to cross-L motion as frequency decreases below the nose. Hence there is a relatively greater sensitivity of the fixed-frequency method to measurement error and also a corresponding need for additional smoothing of the data.

Note on the numerical analysis. Scaled values of τ_n^{-1} are processed by a computer program that compensates for variations in tape-recorder speed. From the appropriately corrected values of τ_n^{-1} new values of τ_n^{-1} spaced at equal intervals of time are obtained by linear interpolation. These values are then smoothed by four successive five-point running means and differentiated by a parabolic fit to each succession of three smoothed points. This procedure was chosen for simplicity in obtaining initial results. A few calculations were made involving least-squares fits to second- and higher-order polynomials, and quite comparable results were obtained. Attempts to find optimum methods are now underway. A report describing the various methods of determining E_w from whistlers is in preparation.

Studies of experimental error have thus far emphasized intercomparison of results from independent paths (Figure 3) and comparison of calculated E_w with other apparently related geophysical quantities (e.g., Figure 4). The resulting preliminary estimate is ±25% accuracy for the data points or curves of Figures 3, 7, and 8, when $|E_w| > 2.0$ mv/m and ±0.05 mv/m and when $|E_w| < 2.0$ mv/m. For results from the fixed-frequency method (Figure 6, lower curves, and Figure 8, dashed curve) these error ranges should be roughly doubled.

DC 'offsets' as limits on accuracy of the method. Protonosphere-ionosphere coupling fluxes and changes in ionospheric electron density introduce apparent convection effects through modification of the electron content in field-aligned tubes of ionization. The magnitudes

of the corresponding effects on whistler travel time vary with L and with the value of the assumed coupling fluxes or ionospheric density variations. For an assumed nighttime downward flux of 1.5×10^8 el/cm^2 sec, based on *Park*'s [1970] whistler measurements, the apparent E_w within the plasmasphere is of the order of 0.04 mv/m at $L = 3$ and 0.01 mv/m at $L = 4$. The values reported in the present paper were adjusted to account for these effects.

Solar illumination of one end of a field line gives rise to an apparent eastward field of the order of 0.01 mv/m at $L \sim 4$ and 0.04 mv/m at $L \sim 3$. Such effects, which would begin near 0800 UT in the events illustrated above, have not been included in the present paper. The basic results of the paper should not be affected by this omission.

Acknowledgments. We are indebted to the organizations and individuals whose many efforts have made possible the Stanford University VLF programs at Eights and Byrd, Antarctica, among them the Office of Polar Programs of the National Science Foundation and the U.S. Navy Support Force. We are grateful for the support and advice of R. A. Helliwell, principal investigator of the Stanford VLF program. For his many efforts we thank John Katsufrakis, supervisor of field activities in the Antarctic for Stanford. We thank Sandee Torgrimson and Donna Craig, who have conscientiously carried out the bulk of the detailed measurements of whistler spectra reported here. We are grateful to S. Akasofu and C. Meng for assistance and comments, to Neil Brice for consistent encouragement, to A. Fraser-Smith for suggestions on power-spectrum analysis, and to many other colleagues for valuable discussions and guidance.

This research was supported in part by the Office of Polar Programs of the National Science Foundation under grant GA-19608, in part by the Atmospheric Sciences Section of the National Science Foundation under grant GA-18129, and in part by National Aeronautics and Space Administration under grant NGL-05-020-008.

* * *

The Editor thanks N. Brice and M. Rycroft for their assistance in evaluating this paper.

REFERENCES

Angerami, J. J., A whistler study of the distribution of thermal electrons in the magnetosphere, *SEL-66-017*, Radiosci. Lab., Stanford Electron. Lab., Stanford Univ., Stanford, Calif., May 1966.

Brice, N. M., and R. L. Smith, Whistlers: Diagnostic tools in space plasma, in *Methods of Experimental Physics*, vol. 9B, Academic, New York, 1971.

Carpenter, D. L., Whistler studies of the plasmapause in the magnetosphere, 1, Temporal variations in the position of the knee and some evidence on plasma motions near the knee, *J. Geophys. Res., 71,* 693, 1966.

Carpenter, D. L., Remarks on the ground-based whistler method of studying the magnetospheric thermal plasma, *Ann. Geophys., 26,* 363, 1970.

Carpenter, D. L., and R. L. Smith, Whistler measurements of electron density in the magnetosphere, *Rev. Geophys. Space Phys., 2,* 415, 1964.

Carpenter, D. L., and K. Stone, Direct detection by a whistler method of the magnetospheric electric field associated with a polar substorm, *Planet. Space Sci., 15,* 395, 1967.

Carpenter, D. L., and K. Stone, Recent whistler research on hydromagnetic motions in the plasmasphere, paper presented at the International Symposium on the Physics of the Magnetosphere, Washington, D.C., September 3–13, 1968.

Carpenter, D. L., K. Stone, and S. Lasch, A case of artificial triggering of VLF magnetospheric noise during the drift of a whistler duct across magnetic shells, *J. Geophys. Res., 74,* 1848, 1969.

Choy, L. W., and R. L. Arnoldy, Field-aligned particle currents near an auroral arc, *J. Geophys. Res., 76,* 8279, 1971.

Cornwall, J. M., Radial diffusion of ionized helium and protons: A probe for magnetospheric dynamics, *J. Geophys. Res., 77,* 1756, 1972.

DeForest, S. E., and C. E. McIlwain, Plasma clouds in the magnetosphere, *J. Geophys. Res., 76,* 3587, 1971.

Ershkovich, A. I., and A. A. Nusinov, On eigen modes excitation of the earth's magnetic tail, *Geomag. Aeron., 11,* in press, 1971.

Helliwell, R. A., *Whistlers and Related Ionospheric Phenomena,* Stanford University Press, Palo Alto, Calif., 1965.

Lezniak, T. W., and J. R. Winckler, Experimental study of magnetospheric motions and the acceleration of energetic electrons during substorms, *J. Geophys. Res., 75,* 7075, 1970.

Maynard, N. C., Electric fields in the ionosphere and magnetosphere, paper presented at the Advanced Study Institute on Magnetosphere-Ionosphere Interaction, Dalseter, Norway, April 14–23, 1971.

McIlwain, C. E., Plasma convection in the vicinity of the geosynchronous orbit, paper presented at the Summer Institute on Earth's Particles and Fields, Cortina, Italy, 1971.

Mozer, F. S., Power spectra of the magnetospheric electric field, *J. Geophys. Res., 76,* 3651, 1971*a*.

Mozer, F. S., Origin and effects of electric fields during isolated magnetospheric substorms, *J. Geophys. Res., 76,* 7595, 1971*b*.

Mozer, F. S., and R. H. Manka, Magnetospheric electric-field properties deduced from simultane-

ous balloon flights, *J. Geophys. Res., 76,* 1697, 1971.

Mozer, F. S., and R. Serlin, Magnetospheric electric-field measurements with balloons, *J. Geophys. Res., 74,* 4739, 1969.

Patel, V. L., Magnetospheric tail as a hydromagnetic waveguide, *Phys. Lett., 26A,* 596, 1968.

Park, C. G., Whistler observations of the interchange of ionization between the ionosphere and the protonosphere, *J. Geophys. Res., 75,* 4249, 1970.

Park, C. G., and D. L. Carpenter, Whistler evidence of large-scale electron-density irregularities in the plasmasphere, *J. Geophys. Res., 75,* 3825, 1970.

Park, C. G., and C.-I. Meng, Vertical motions of the midlatitude F_2 layer during magnetospheric substorms, *J. Geophys. Res., 76,* 8232, 1971.

Smith, R. L., The use of nose whistlers in the study of the outer ionosphere, *Tech. Rep. 6,* Radiosci. Lab., Stanford Electron. Lab., Stanford Univ., Stanford, Calif., July 1960.

Smith, R. L., Propagation characteristics of whistlers trapped in field-aligned columns of enhanced ionization, *J. Geophys. Res., 66,* 3699, 1961*a*.

Smith, R. L., Properties of the outer ionosphere deduced from nose whistlers, *J. Geophys. Res., 66,* 3709, 1961*b*.

Smith, R. L., R. A. Helliwell, and I. W. Yabroff, A theory of trapping of whistlers in field-aligned columns of enhanced ionization, *J. Geophys. Res., 65,* 815, 1960.

(Received November 12, 1971;
accepted March 2, 1972.)